Suppression of the pedestal in a chirped-pulse-amplification laser

Y.-H. Chuang, D. D. Meyerhofer, S. Augst, H. Chen, J. Peatross, and S. Uchida

Laboratory for Lasers Energetics, University of Rochester, 250 East River Road, Rochester, New York 14623-1299

Received June 11, 1990; accepted February 21, 1991

The pedestal (prepulse and postpulse) associated with a chirped-pulse-amplification (CPA) laser is studied. Four components have been identified that contribute to the pedestal. Pulses are spectrally shaped by gain narrowing in a frequency-matched, regenerative amplifier, while self-phase modulation is avoided. The intensity contrast is further improved through the use of a saturable absorber, resulting in Gaussian pulses of ~0.9-ps duration with an intensity contrast exceeding 10^5:1. Both experimental and numerical descriptions of these processes are presented. This investigation makes possible the study of high-intensity ultrashort laser–plasma interactions with a fiber–grating CPA system.

1. INTRODUCTION

The study of high-density plasma physics[1] and ultrafast x-ray emission[2,3] by means of high-power, ultrashort laser pulses is of great current interest. Detailed knowledge of the temporal shape of the pulse is crucial. In particular, high-density plasma physics experiments require a laser pulse with a high-intensity contrast. The peak intensity may be well above 10^{16} W/cm^2, whereas the prepulse intensity should be limited to ~10^{11} W/cm^2 if one is to avoid generating a low-density, preformed plasma. In this paper we report the generation of 0.9-ps Gaussian laser pulses with intensity contrasts exceeding 10^5 by means of a chirped-pulse-amplification (CPA) laser system.

CPA laser systems permit the production of high-power, ultrashort pulses in solid-state lasing media.[4] A laser pulse from a mode-locked oscillator is frequency chirped, temporally expanded in a fiber, and further stretched in time by an expansion-grating pair. The longer pulse permits more energy to be extracted from the subsequent amplifier system than would a short pulse. After amplification the pulse is compressed to picosecond or subpicosecond duration by a grating pair. There is a resulting increase in power that is equal to the chirp ratio, the stretched-pulse duration divided by the compressed-pulse duration. The generation of the frequency chirp in the fiber, the compression- and the expansion-grating pairs, and the chirp ratio are well described in Refs. 5, 6, 7, and 8, respectively.

It is well known that the fiber–grating compression technique produces a pulse that carries a significant amount of energy and remains imperfectly compressed. This uncompressed portion is commonly referred to as the pedestal. Pedestal reduction is discussed in many papers. Nonlinear birefringence can cause a fiber to act as an intensity discriminator and partially suppress the pedestal.[9] Careful adjustment of the compression gratings can help to reduce the third-order nonlinear chirp that arises from the fiber.[10] Spectral windowing[11] can nearly eliminate the pedestal, but the temporal shape of the pulse may still not be Gaussian. Recently Perry *et al.*[12] used the gain narrowing of the regenerative amplifier to do spectral shaping in a CPA system. They successfully shaped the spectrum to a near-Gaussian form, making the pulse also near Gaussian. For this technique an intensity contrast of greater than 700:1 was reported.

This paper explores the pedestal that is associated with a CPA laser. Four components have been identified that contribute to the pedestal of a compressed pulse. Two effects originate in the regenerative amplifier: (a) a large, 200-ps background pedestal that is due to self-phase modulation (SPM) and gain saturation and (b) étalon effects. The nonlinear frequency chirp and square-top pulse envelope that are generated in the optical fiber lead to the other two effects: (c) pulse wings that make the pulse wider than a true Gaussian at low intensities[13,14] and (d) satellite pulses that are 80 ps from the main pulse. Low-intensity, long-duration satellite pulses are a result of a negative frequency chirp[15] or an unshifted frequency component.[16] The pedestal contributions of the regenerative amplifier are removed by operation below saturation, removal of étalon effects, and adjustment of the line center to that of the chirped pulse after the fiber. The pulse wings are suppressed by spectral gain narrowing in the regenerative amplifier,[12] and the satellite pulses are suppressed by a saturable absorber. Gaussian pulses of durations less than 0.9 ps with intensity contrasts exceeding 10^5:1 have been produced. This investigation makes possible the study of high-intensity ultrashort laser–plasma interactions with a fiber–grating CPA system. In Section 2 the current CPA laser system is introduced. Section 3 presents experiments on pedestal suppression. Numerical calculations of the effects of gain narrowing, frequency mismatch between the oscillator and the regenerative amplifier, and SPM are discussed in Section 4. This paper is summarized in Section 5.

2. LASER SYSTEM AND EXPERIMENTAL SETUP

A schematic diagram of the current CPA laser system is shown in Fig. 1. It consists of three parts: the pulse-preparation stage, the amplifier chain, and the compression stage. Figure 1(a) shows the pulse-preparation stage.

0740-3224/91/061226-10$05.00

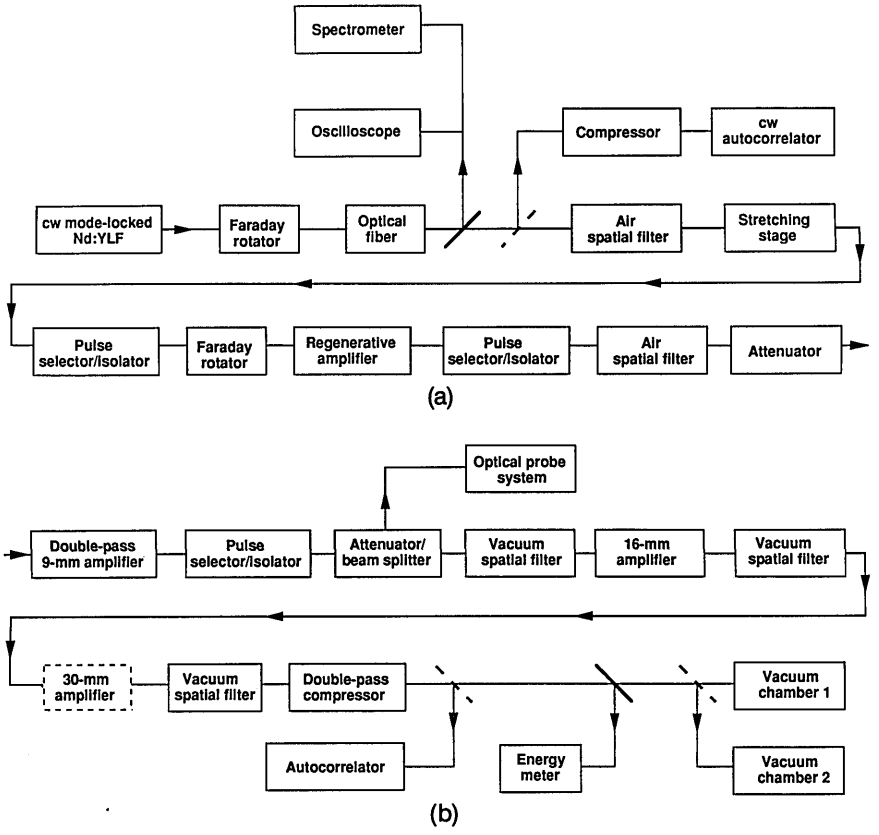

Fig. 1. Schematic diagram of the current CPA laser system. (a) Pulse-preparation stage. The regenerative amplifier serves to amplify and to shape the laser pulse. (b) Amplifier chain and compression stage.

A cw-pumped, mode-locked Nd:YLF oscillator generates a 100-MHz train of 50-ps pulses at a wavelength of 10 530 Å. The pulses are coupled into a 0.8-km single-mode optical fiber with a 9-μm core and then are sent through a pair of expansion gratings. The pulse undergoes SPM and group-velocity dispersion in the fiber and further dispersion by the expansion-grating pair. This leads to chirped pulses with 37-Å bandwidths and 300-ps durations. A cw autocorrelator monitors the compressibility of the chirped pulses produced in the fiber. A small grating pair, matched to the high-power compression gratings, is used to compress the pulse.

A single nanojoule energy-level pulse is selected by a Pockels cell and seeded into a Q-switched, end-mirror-dumped regenerative amplifier. The amplifier uses a 7-mm-diameter phosphate ND:glass rod (Kigre Q98). (A carefully designed regenerative amplifier not only amplifies the laser pulse but also shapes the laser spectrum.[12] For this reason the regenerative amplifier is considered part of the pulse-preparation stage.) A 1-mJ pulse is selected from the pulse train, which is transmitted through the 50% reflective end mirror in the regenerative amplifier. The spatial profile of the beam is improved with an air spatial filter. An attenuator that consists of a half-wave plate between two polarizers is used to control the energy put into the amplifier chain.

The amplifier chain and the compression stage are shown in Fig. 1(b). All the amplifiers contain Nd:glass with a maximum gain at 10 530 Å. The amplifier chain consists of a double-pass 9-mm-diameter amplifier (Kigre Q-98, 235 mm long) and a single-pass 16-mm-diameter amplifier (Hoya LHG-8, 360 mm long). A single-pass 30-mm-diameter amplifier (Hoya LHG-8, 360 mm long) is added when compression gratings with a higher damage threshold are installed. One Pockels cell after the 9-mm amplifier further isolates the pulse and suppresses any feedback pulse that might result from reflections off optical elements. An additional attenuator increases the system's dynamic range to 10^6. A vacuum spatial filter after each amplifier is used to upcollimate, to relay the image, and to filter the pulse spatially. The energy of the chirped pulse after the 16-mm amplifier can be as high as a joule, with a repetition rate of 1 shot per 70 s (limited by the thermal lensing in the 16-mm amplifier rod).

The compression stage currently consists of two 1700 line/mm gold-coated holographic gratings with dimensions of 80 mm × 110 mm. The gratings are used in the near-Littrow, double-pass configuration with a separation distance of 164 cm. The laser pulse is compressed to 1.6 ps with a bandwidth of 13.5 Å when no saturable absorber is used. The laser beam has a 36-mm diameter, currently limiting the maximum energy to 300 mJ because of the damage threshold of the compression gratings. An autocorrelator and an energy meter are used to measure the final pulse width and pulse energy after compression.

The laser spectrum and pulse width are almost unaffected by our amplifier chain (after the regenerative amplifier) because of the relatively low amount of gain compared with that in the regenerative amplifier. For the experiments on pedestal suppression the laser pulse goes directly from the pulse-preparation stage to the compressor. This allows the laser to operate at a repetition

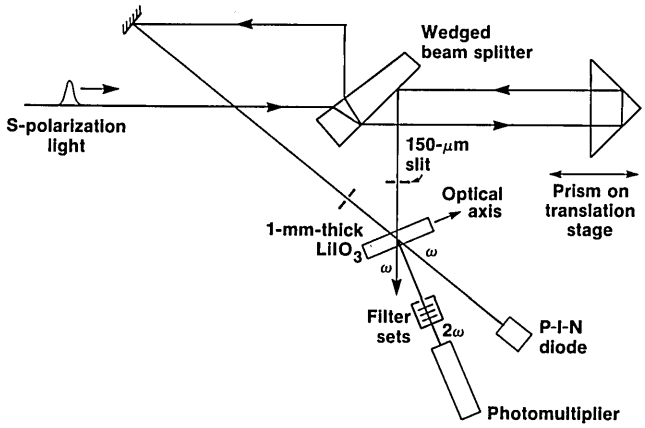

Fig. 2. Autocorrelator. The wedged beam splitter and slits are used to prevent all étalon reflections from reaching the photomultiplier. The P-I-N diode detects shot-to-shot laser energy fluctuations. This setup becomes a single-shot autocorrelator when the slits are removed and the photomultiplier is replaced by a linear-array detector.

rate of 1 Hz. The main diagnostic for this experiment is an autocorrelator, as shown in Fig. 2. The wedged beam splitter and slits are used to prevent all secondary reflections within the autocorrelator from reaching the photomultiplier. The P-I-N diode measures shot-to-shot laser energy fluctuations. The autocorrelation signal is obtained by division of the photomultiplier signal by the square of the P-I-N diode signal. This assumes a nondepletion condition for second-harmonic generation. Each data point in the autocorrelation trace represents an average over 10 shots. The standard deviation is shown by the error bars. This setup becomes a single-shot autocorrelator when the slits are removed and the photomultiplier is replaced by a linear-array detector. We use this single-shot autocorrelator to begin the initial pulse-width measurement and to align the compression gratings and then use multiple shots to obtain a detailed autocorrelation trace.

3. EXPERIMENTS ON PEDESTAL SUPPRESSION

Improvements in the laser-pulse shape begin with a careful adjustment of the regenerative amplifier in order to avoid gain-saturation, SPM, and étalon effects. Next the gain narrowing of the frequency-matched regenerative amplifier shapes the pulse wings.[12] Finally, a saturable absorber suppresses the satellite pulses.

A. Background Pedestal Induced in the Regenerative Amplifier

The end-mirror-dumped regenerative amplifier produces a train of pulses, one of which is selected for injection into the amplifier chain. Pulses were sampled at various times with respect to saturation, and it was found that pulses near saturation are strongly spectrum modulated. The distortion in the pulse appears to be due to the combination of SPM[17] with a mismatch in the gain-center wavelength of the regenerative amplifier and the Nd:YLF oscillator. This effect will be discussed in Section 4. Figure 3(a) shows the autocorrelation trace of a compressed pulse that was extracted at the saturation level of the regenerative amplifier. The bandwidth of the injected chirped pulse was only 20 Å, and there was a frequency mismatch of 4 Å between the line center of the chirped pulse and that of the regenerative amplifier. An overwhelming 200-ps-long background pedestal is generated. One can reduce this type of pedestal by switching a pulse out from the train before the regenerative amplifier reaches its saturation level. This would reduce the total B integral[8] seen by the pulse. Figure 3(b) shows the autocorrelation trace of the compressed pulse, which is 5 pulses (~50 ns) earlier than the peak of the pulse train. The Gaussian-curve fits in Fig. 3 show the ideal pulses, the goal of this experiment.

A further improvement involved adjustment of the Brewster-plate angle and the Q-switch voltage inside the regenerative amplifier cavity in order to match the spectral line center of the Q-switched pulse to that of the seed pulse. In addition, étalon effects were removed through the use of wedged optics.

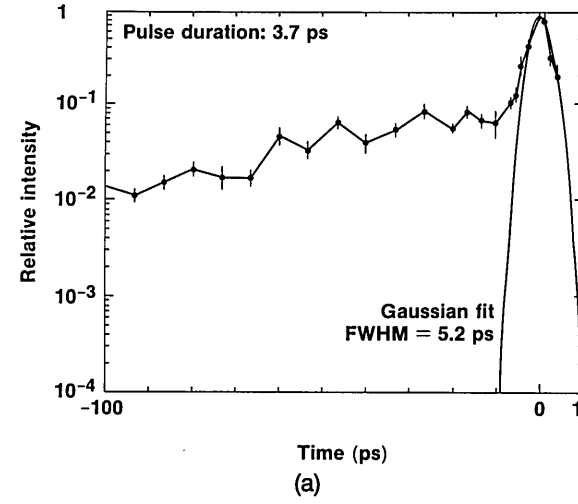

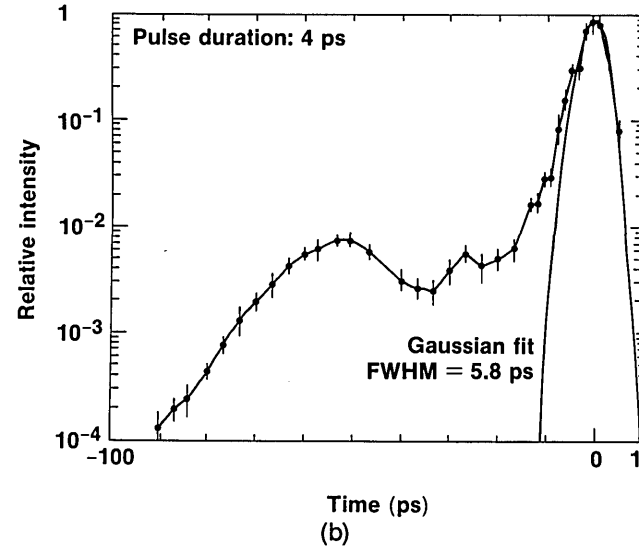

Fig. 3. Autocorrelation traces of the compressed pulse with various contributions to the pedestal. (a) A compressed pulse with the regenerative amplifier operating at saturation shows the overwhelming background pedestal. (b) Below saturation other pedestal structures are shown; the Gaussian-curve fits show the ideal pulses. Each data point represents the average of 10 shots.

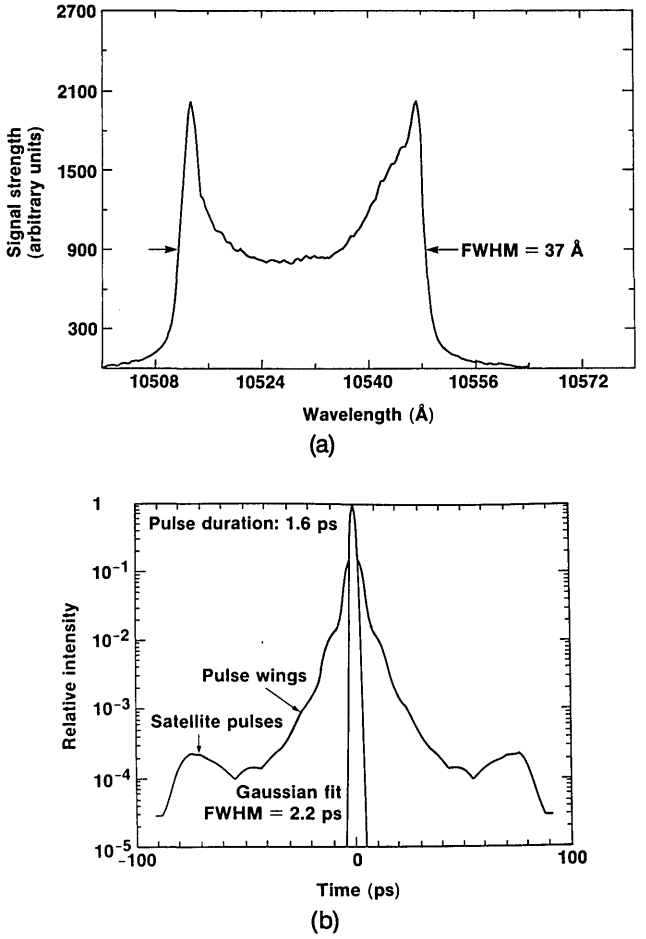

Fig. 4. (a) Spectrum of the chirped pulse leaving the fiber, FWHM 37 Å. (b) Autocorrelation trace of the compressed pulse without amplification, FWHM 1.6 ps, assuming a Gaussian profile. This figure shows that the pulse wings and the satellite pulses are the results of imperfect fiber chirping.

B. Pulse Wings

The pulse wings of a compressed pulse come from the nonlinear chirp and the square-top envelope that are generated in the fiber.[13,14] A typical power spectrum of a chirped pulse after the fiber in our laser system is shown in Fig. 4(a). The bandwidth is 37 Å, and the line center is at 10530 Å, the wavelength of our Nd:YLF oscillator. The results reported in Ref. 13 show that the linear chirp is located near the center part of the spectrum, while the nonlinear chirp is located near the wings. There can be additional nonlinear chirps associated with the expansion- and compression-grating pairs.[18] Figure 4(b) shows the autocorrelation trace of the compressed pulse after the fiber without further amplification. This figure clearly shows the side effects of the nonlinear chirp, a 1.6-ps pulse with broad pulse wings. An additional feature that can be seen in Fig. 4(b) is the long satellite pulses that are due to negative frequency chirp and frequency-unshifted light.

There are many methods that can be used to reduce the pulse wings. Spectral windowing[11] can be used within the expansion gratings. A bandpass filter can be used to remove the nonlinear chirp. One can also remove the nonlinear chirp by adjusting the angle of incidence and separation distances between the compression gratings, though this can lead to astigmatism in the compressed pulse.[19]

For our system we found gain narrowing in the spectrally line-center-matched regenerative amplifier to be the best choice for spectral windowing.[12] The laser spectrum is forced to become Gaussian, leading to a temporally Gaussian compressed pulse. The spectrum of a pulse switched out of the regenerative amplifier with a bandwidth of 13.5 Å is shown in Fig. 5(a). The corresponding autocorrelation trace of the compressed pulse with a width of 1.6 ps is shown in Fig. 5(b). The pulse profile is nearly Gaussian for 3 orders of magnitude. Low-intensity, long-duration satellite pulses are clearly shown. With this spectral-shaping scheme the final problem is the elimination of the last structure in the pedestal, i.e., the satellite pulses.

C. Low-Intensity, Long-Duration Satellite Pulses

There are two low-intensity, long-duration satellite pulses. We have used the third-order correlation technique[20] to find that these two satellite pulses are almost symmetrically located at 80 ps on either side of the main peak with an intensity contrast of the order of 10^3. This part of the pedestal originates from the low-intensity wings of the oscillator pulse that either receive a negative frequency chirp in the fiber[15] or go directly through the fiber without SPM.[16] The satellite-pulse intensities decrease when the power spectrum generated by SPM in the fiber is made broader.

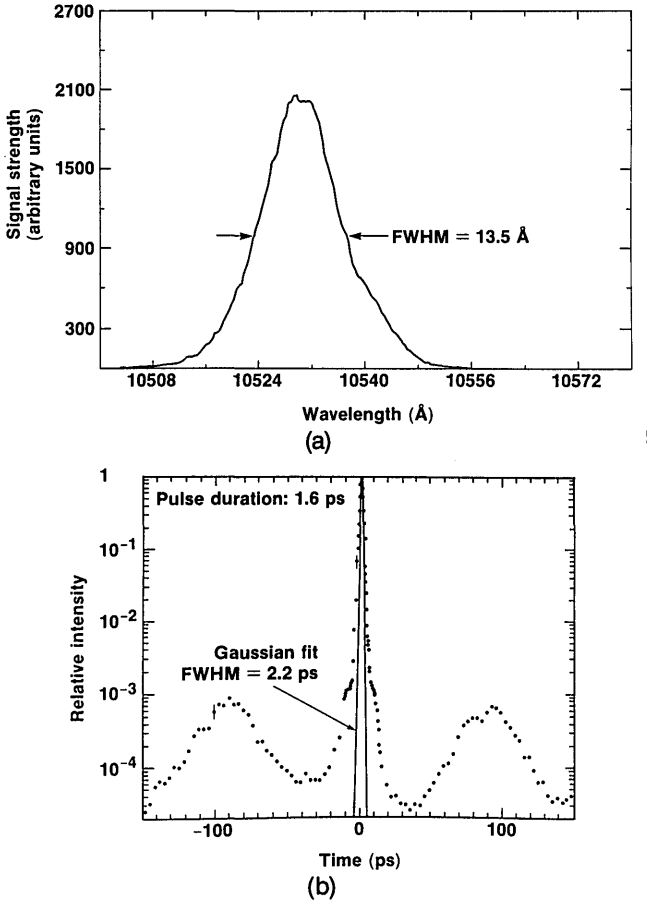

Fig. 5. (a) Spectrum of the pulse leaving the regenerative amplifier, FWHM 13.5 Å. The spectral line center is the same as in Fig. 4(a). (b) Autocorrelation trace of the compressed pulse, FWHM 1.6 ps, assuming a Gaussian profile.

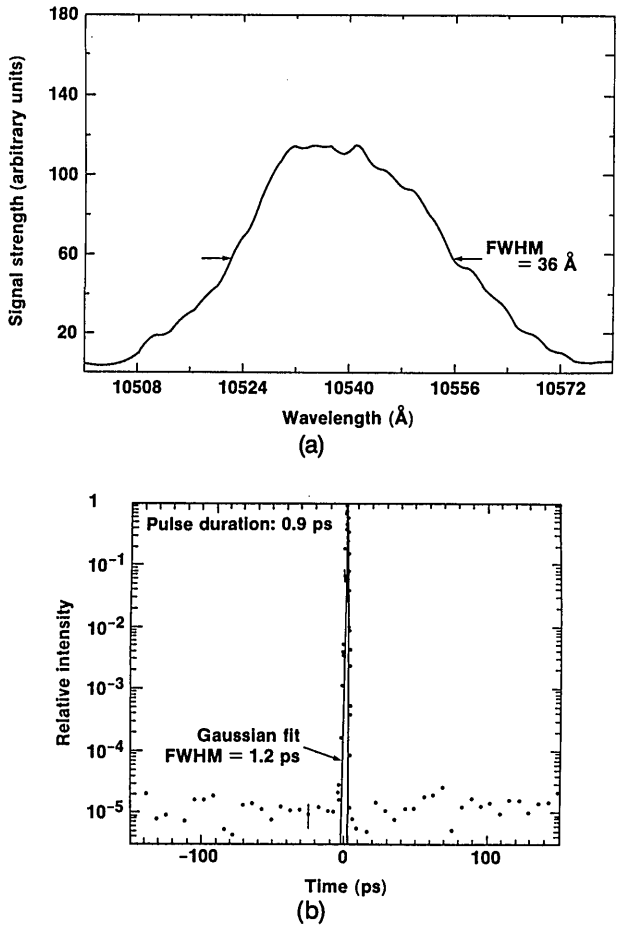

Fig. 6. (a) Spectrum of the pulse with a saturable absorber in the system, FWHM 36 Å. (b) Autocorrelation trace of the compressed pulse, FWHM 0.9 ps, assuming a Gaussian profile. The baseline represents the noise level of our detector and data-acquisition system. The intensity contrast is now greater than 10^5, the limit of our autocorrelator dynamic range.

Saturable absorbers[21] are used to eliminate the low-intensity satellite pulses. Two kinds of saturable absorber are used in this experiment, Kodak Q-switching dyes #9860 and #5. Dye #9860, with pure nitrobenzene as a solvent (approximately 5×10^{-5} M), is contained in a 2-cm-long dye cell. The relaxation time of this saturable absorber is 4.2 ps, which is much shorter than the time delay between the satellite pulses and the main peak. This dye cell is placed between two lenses (f = 140 mm) after the compression gratings, so the peak laser intensity will exceed the saturation intensity of the dye. The low-intensity transmission is less than 10^{-4}, while the transmission for the main peak is ~30%. Figure 6 shows the experimental results with this dye cell in the system (compare it with Fig. 5, without the saturable absorber). The spectrum is broadened to 36 Å and is mainly red shifted, as is shown in Fig. 6(a). The autocorrelation trace of a 0.9-ps pulse, with a Gaussian fit over 5 orders of magnitude, is shown in Fig. 6(b). The satellite pulses are no longer present in this autocorrelation trace. The baseline is the noise from the detector. The intensity contrast is now greater than 10^5, with this valued limited by the dynamic range of our autocorrelator. A rescaled autocorrelation trace of Fig. 6(b) with a Gaussian fit is shown in Fig. 7.

The dye cell is currently placed after the compression gratings with the whole amplifier system firing and is used only when a high-intensity-contrast pulse is required. A 200-cm lens was used to measure the focal characteristics of the beam both with and without the saturable absorber in place. The focal-spot area was larger by approximately a factor of 2 with the saturable absorber in place. This decrease in focusability is probably due to nonuniformities in the near-field pattern of the beam entering the saturable absorber. The nonlinearity of the saturation process can enhance the nonuniformities. It is also possible that self-focusing, which also degrades the focal spot, accompanies the SPM. The factor-of-2 degradation of the focal-spot area appears to be an acceptable trade-off for the improved temporal quality.

The second saturable absorber, dye #5 with 1,2-dichloroethane as the solvent (approximately 5×10^{-5} M), is contained in a 1-cm dye cell. The relaxation time of this saturable absorber is 2.7 ps, which is even shorter than that of dye #9860. This dye cell is put in the same position as the dye #9860. The low-intensity transmission is less than 10^{-4}, while the transmission for the main peak is ~30%. The experimental result had the same characteristics as those for dye #9860 except the pulse width was slightly longer at 1.1 ps.

4. MODELING OF THE CHIRPED-PULSE AMPLIFICATION

We performed a series of calculations in order to understand the modifications of the chirped pulse in the regenerative amplifier. We found that SPM can play an important role in determining the final shape of the compressed pulse even at relatively low values of the total B integral. The calculations are summarized in Subsection 4.A, but the details are left to a future publication.[22] In Subsection 4.B the results of the calculations are shown.

A. Model

This model is based on time-domain analysis. The instantaneous frequency, defined as the time derivative of the light-field phase, is used as an approximation of Fourier-transform frequency to simplify the analysis. The validity of this approximation is based on the assumption that the time scale of the envelope variation of the laser pulse is much longer than the dephasing time of

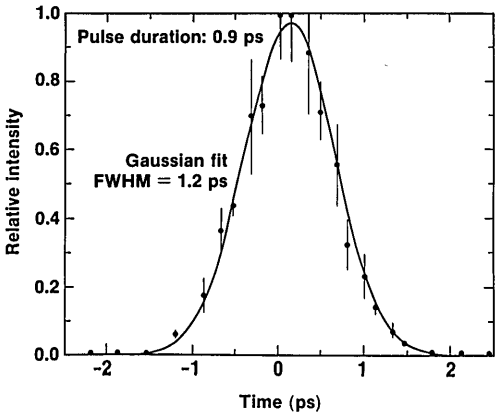

Fig. 7. Rescaled view of Fig. 6(b). A detailed autocorrelation trace of a 0.9-ps pulse with a Gaussian fit is shown.

the gain medium.[22] Within this model the following topics are investigated: (a) the spectral gain-narrowing effect in the amplification process, (b) SPM induced by the amplifier, (c) the results of the frequency mismatch between the seeding pulse and the gain profile of the amplifier, and (d) pulse compression and the resulting pedestal.

The model incorporates a laser pulse, $E(z,t) = E_0(z,t)\exp\{i[\omega_0 t + \phi_m(t)]\}$, traveling in the $+z$ direction through a gain medium with a small-signal power-gain coefficient $\alpha(\omega)$. The time derivative of the phase variation $\phi_m(t)$ describes the frequency chirp of the input pulse. We neglect dispersion effects and transverse intensity variations in order to simplify the analysis. Since preserving the initial pulse frequency chirp is necessary for a CPA laser, the role of SPM becomes important. The nonlinear dependence of the index of refraction on the applied signal strength is given by the optical Kerr effect, $n = n_0 + n_{2E}\langle E^2\rangle = n_0 + n_{2E}|E_0|^2/2 = n_0 + n_2 I$. The basic equation that governs the light propagation in an amplifier, including SPM, is[22]

$$\frac{\partial E_0(z,t)}{\delta z} = \frac{\alpha(\omega_i)}{2}E_0(z,t) - i\frac{\beta_2}{2}|E_0|^2 E_0(z,t), \tag{1}$$

where $\beta_2 = 2\pi n_{2E}/\lambda_0$ and λ_0 is the laser wavelength in vacuum. Note that z and t refer to coordinates in the moving pulse frame, which is defined by the transformation $z = \hat{z}$ and $t = \hat{t} - \hat{z}/c$, where $\hat{z}$ and $\hat{t}$ are ordinary laboratory coordinates and c is the velocity of light in the amplifier. The instantaneous frequency is defined by $\omega_i(t) \equiv \delta\phi_{\text{tot}}/\delta t$, where ϕ_{tot} is the total field phase variation. When the SPM is still small, such that the instantaneous frequency $\omega_i(t)$ can be approximated by $\omega_0 + \mathrm{d}\phi_m(t)/\mathrm{d}t$ with no z dependence, Eq. (1) can be solved to yield[5]

$$E_0(z,t) = E_0(0,t)\exp\left[\frac{\alpha(t)z}{2}\right]\exp[-i\phi_{\text{SPM}}(z,t)], \tag{2}$$

with the phase modulation

$$\phi_{\text{SPM}}(z,t) = 1/2[\beta_2/\alpha(t)]|E_0(0,t)|^2\{\exp[\alpha(t)z] - 1\}, \tag{3}$$

where $\alpha(t)$ is short for $\alpha[\omega_i(t)]$. Equation (3) is nothing but the result of the B integral with time dependence. For a multiple-pass amplifier with a single-pass power gain equal to $G(t) \equiv \exp[\alpha(t)L]$, where L is the length of the laser amplifier, and a power loss equal to $1 - R$, the laser field is amplified M times, to become

$$E_0(t) = E_0(0,t)[RG(t)]^{M/2}\exp[-i\phi_{\text{SPM}}(t)], \tag{4}$$

with

$$\phi_{\text{SPM}}(t) = \frac{1}{2}\frac{\beta_2}{\alpha(t)}|E_0(0,t)|^2[G(t) - 1]\frac{[RG(t)]^M - 1}{RG(t) - 1}. \tag{5}$$

1. Gain Narrowing

To explain pulse shaping by the spectral gain-narrowing effect, we begin from Eq. (4) with an initial laser pulse that has a super-Gaussian envelope and a phase modulation $\phi_m(t) = \frac{1}{2}b(t/\tau)^2 + \phi_{NL}(t)$. This choice provides a good model for the measured chirped-frequency spectrum, which is injected into the regenerative amplifier. For simplicity the low-intensity, long-duration satellite pulses (see Subsection 3.C) are neglected in the model because they are unaffected by gain narrowing and SPM. The parameter b defines the linear chirp, and the phase variation $\phi_{\text{NL}}(t)$ represents the possible nonlinear frequency chirp, $O[(t/\tau)^3]$. The injected laser pulse is

$$E(0,t) = A_1\exp\left[-\frac{1}{2}\left(\frac{t}{\tau}\right)^{2m}\right] \times \exp\left\{i\left[\omega_0 t + \frac{1}{2}b\left(\frac{t}{\tau}\right)^2 + \phi_{\text{NL}}(t)\right]\right\}, \tag{6}$$

where the number m is determined by the rise time of the real pulse,[5] which can be estimated by $\tau_r \equiv \tau/m$. The instantaneous frequency is $\omega_i(t) = \omega_0 + bt/\tau^2 + O[(t/\tau)^2]/\tau$. When the bandwidth of the applied signal is much smaller than that of the gain profile, the gain coefficient can be simplified by a quadratic form, $\alpha[\omega_i(t)] = \alpha_0 - (\alpha''/2)[\omega_i(t) - \omega_a]^2 \approx \alpha_0 - (\alpha''/2)(\omega_0 + bt/\tau^2 - \omega_a)^2$, where $\alpha'' = -\mathrm{d}^2\alpha(\omega)/\mathrm{d}\omega^2$ when evaluated at the midband frequency ω_a. Then, for the frequency-matched case, $\omega_0 = \omega_a$, Eq. (4) becomes

$$E(t) = A_2\exp\left[-\frac{1}{2}\left(\frac{t}{\tau}\right)^{2m} - \frac{1}{2}\left(\frac{t}{\tau_{\text{eff}}}\right)^2\right] \times \exp\left\{i\left[\omega_0 t + \frac{1}{2}b\left(\frac{t}{\tau}\right)^2 + \phi_{\text{NL}}(t) - \phi_{\text{SPM}}(t)\right]\right\}, \tag{7}$$

where $A_2 \equiv A_1(RG_0)^{M/2}$ is the amplitude at the midband after amplification, with $G_0 \equiv \exp(\alpha_0 L)$, the single-pass power gain at midband, and $\tau_{\text{eff}} \equiv (2\tau^4/M\alpha'' Lb^2)^{1/2}$ represents the shortened half-width of the chirped pulse. The phase variation $\phi_{\text{SPM}}(t)$ is evaluated by means of Eq. (5), with $G(t) = G_0\exp[-1/m(t/\tau_{\text{eff}})^2]$.

Suitable pulse shaping is accomplished when $\tau > \tau_{\text{eff}}$; that is, the sharp edges of the super-Gaussian pulse and the unwanted phase variation near the edges, $\phi_{\text{NL}}(t)$, are suppressed by the Gaussian gain curve. With the reasonable approximations $b \approx \tau\Delta\omega_L/2$ and $\alpha'' \approx 8\alpha_0/(\Delta\omega_a)^2$, which is exact for a Lorentzian gain profile, the inequality becomes

$$M\alpha_0 L > (\Delta\omega_a/\Delta\omega_L)^2, \tag{8}$$

where $\Delta\omega_L$ is the full bandwidth of the laser pulse and $\Delta\omega_a$ is the atomic linewidth of the gain medium. This equation shows the condition (lower bound) for a significant gain-narrowing effect as a pulse-shaping tool in the amplifier. In this case we can drop the super-Gaussian term in Eq. (7). If SPM is still negligible, the applied signal becomes a complex Gaussian pulse,[8] which can then be compressed to a Fourier-transform-limited pulse with a half-width (at $1/e$ intensity point) approximately equal to $(\tau/\tau_{\text{eff}})(\tau/b)$ in the large-chirp limit $b/(\tau^2 \gg 1/\tau_{\text{eff}})^2 \gg 1$. The factor τ/τ_{eff} is the pulse-broadening ratio for the compressed pulse, which is equal to the pulse-shortening ratio of the chirped pulse in the amplifier that is due to the gain-narrowing effect. The power spectrum of this Gaussian pulse in the large-chirp assumption is proportional to $\exp[-(\tau^4/b^2\tau_{\text{eff}}^2)(\omega - \omega_0)^2] = \exp[-\frac{1}{2}M\alpha'' L(\omega - \omega_0)^2]$, which is exactly the line shape $G(\omega)^M$, as expected.[12]

2. Self-Phase Modulation

SPM of the laser pulse that is induced by the amplifier host material generates extra phase variation, $\phi_{\text{SPM}}(t)$.

SPM is most important when the laser operates near saturation, where it has the largest intensity. The new frequency chirp, $\Delta\omega_{SPM} = -\partial\phi_{SPM}/\partial t$, adds to the original linear frequency chirp of the laser pulse and changes the laser power spectrum. This new frequency chirp has a different group delay from the original chirp and hence adds a pedestal to the compressed pulse. Before saturation the calculated ϕ_{SPM} can be obtained from Eq. (5). Near saturation we can use the small-gain approximation, $z = L$, $\exp[\alpha(t)L] \approx 1 + \alpha(t)L$ (small gain), and $\frac{1}{2}n_{2E}|E(0,t)|^2 = n_2 I$ in Eq. (3). The induced SPM in the amplifier (one trip) is $\phi_{SPM}(t) = 2\pi n_2 I(t)L/\lambda_0$. The new added frequency chirp is $\Delta\omega_{SPM}(t) = -(2\pi n_2 L/\lambda_0)\partial I(t)/\partial t$. Gain narrowing in the amplifier has a significant effect on the pulse shape. From the results of Eq. (7), the additional frequency chirp, evaluated at $t = \tau$ after a single pass through the amplifier, is given for $m \gg 1$ by

$$\Delta\omega_{SPM} = 0.74\left[m + \left(\frac{\tau}{\tau_{eff}}\right)^2\right]\exp\left[-\left(\frac{\tau}{\tau_{eff}}\right)^2\right]\frac{\Phi_{max}}{\tau}, \qquad (9)$$

where $\phi_{max} \equiv 2\pi n_2 I_0 L/\lambda_0$, and I_0 is the peak laser intensity. For a pulse with a Gaussian envelope of width τ_{eff}, for example, one that has undergone gain narrowing, the maximum frequency chirp is $\Delta\omega_{SPM} = 0.86\,\Phi_{max}/\tau_{eff}$ evaluated at $t = \tau_{eff}/2^{1/2}$, the point of maximum $\partial I/\partial t$.

In a regenerative amplifier the transverse mode of the laser pulse is confined to the lowest-order, or 00, mode. Transverse variations of the laser pulse cause different SPM's at each transverse position.[17] Since our purpose is to avoid SPM in the amplification process, the peak intensity near the beam-axis is most important.

3. *Frequency Mismatch*

If a frequency mismatch exists between the seed pulse and the gain profile of the amplifier, i.e., $\omega_0 \neq \omega_a$, one of the sharp edges of the super-Gaussian pulse (which also carries higher-order nonlinear chirp) cannot be suppressed efficiently through gain narrowing. Thus the pulse shaping is poor, and SPM remains strong at the sharp edge. To avoid SPM, we must lower the energy extraction efficiency in the amplifier. The power gain in this case is given by

$$G(t) = G_0^M \exp\left[-M\frac{\alpha''L}{2}\left(\frac{bt}{\tau^2} + \omega_0 - \omega_a\right)^2\right]$$
$$= G_0^M \exp\left[\frac{-(t - t_0)^2}{\tau_{eff}^2}\right], \qquad (10)$$

where $t_0 = \tau^2(\omega_a - \omega_0)/b \approx 2(\omega_a - \omega_0)\tau/\Delta\omega_L$.

4. *Pulse Compression and Pedestals*

The Fourier transform of a linearly chirped pulse $A(t)\exp\{i[\omega_0 t + \frac{1}{2}b(t/\tau)^2]\}$ is

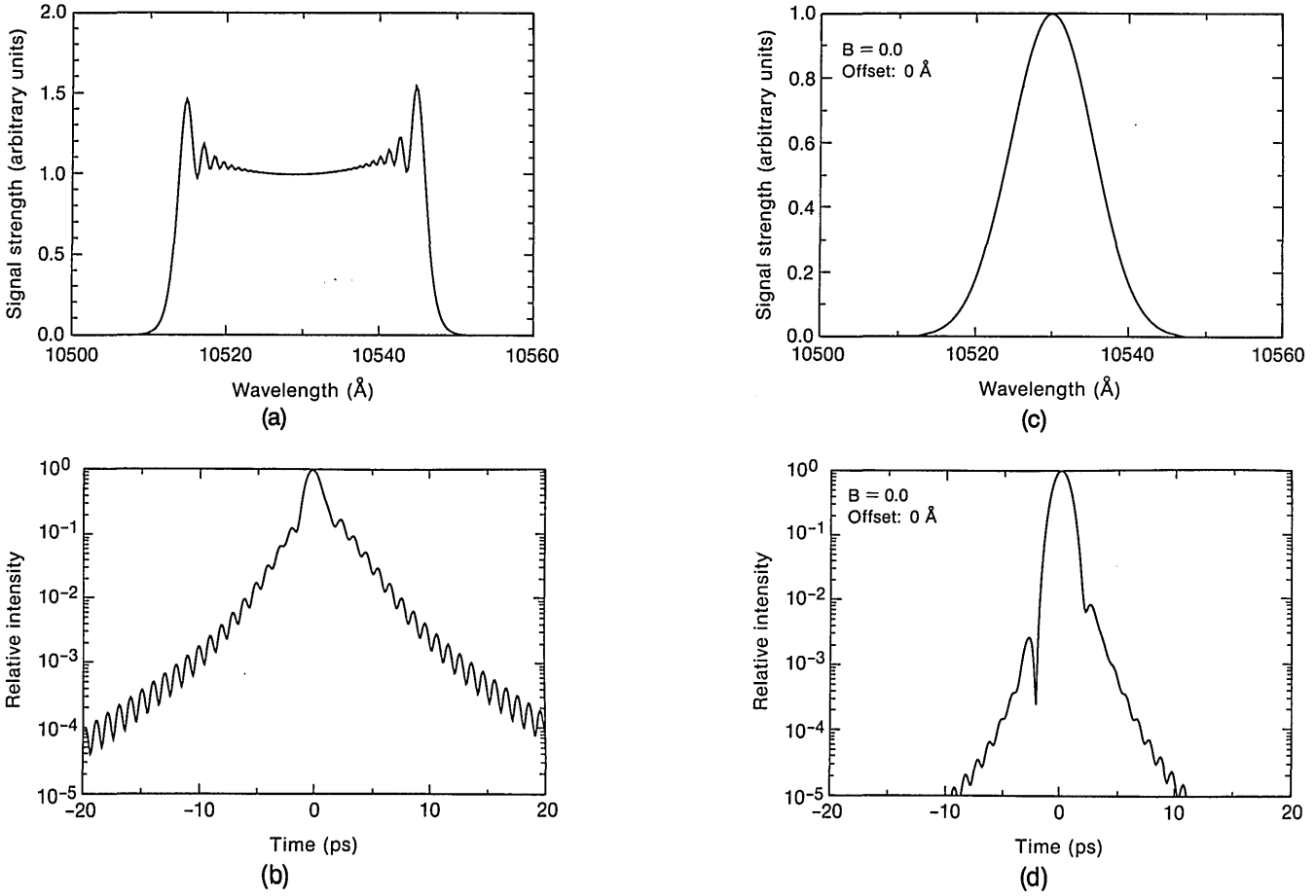

Fig. 8. Model calculations, showing the frequency spectrum and compressed-pulse shape (a), (b) before and (c), (d) after gain narrowing in the regenerative amplifier. The initial bandwidth is 37 Å with a chirped-pulse duration of (a), (b) 150 ps, stretched to (c), (d) 300 ps before amplification.

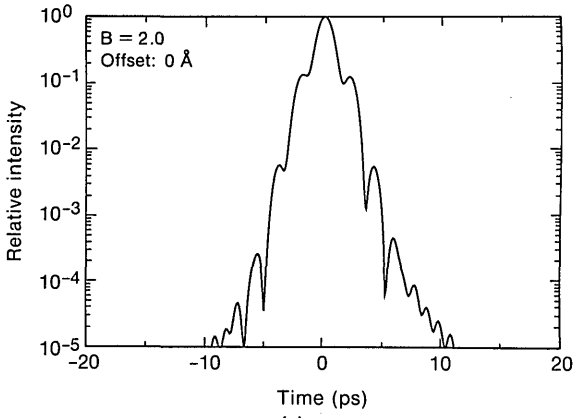

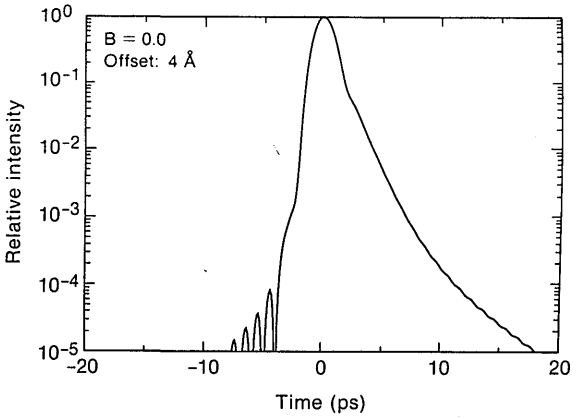

Fig. 9. Effect of frequency mismatch ($\Delta\lambda$) and SPM (B) on the compressed pulse shown in Fig. 8. (a) $\Delta\lambda = 0$ Å, $B = 2$, (b) $\Delta\lambda = 4$ Å, $B = 0$.

$$\int A(t)\exp\left\{i\left[\omega_0 t + \frac{1}{2}b\left(\frac{t}{\tau}\right)^2\right]\right\}\exp(-i\omega t)\mathrm{d}t$$
$$= \exp\left(\frac{-i\omega'^2 t^2}{2b}\right)\int A(t)\exp\left[i\left(\frac{b}{2}\right)\left(\frac{t}{\tau} - \frac{\omega'\tau}{b}\right)^2\right]\mathrm{d}t, \quad (11)$$

where ω' is short for $\omega - \omega_0$. The integral on the right-hand side of Eq. (11) has a form similar to Huygens's integral in the Fresnel diffraction approximation with $b = 2\pi N_f$, where N_f is the Fresnel number. Thus the power spectrum of the chirped pulse can be understood with an analogy to diffraction.[22] For a large-chirp pulse, pulse compression is performed with a pair of gratings that are used to eliminate the phase term, $\exp[-i\omega'^2\tau^2/(2b)]$, in front of the integral on the right-hand side of Eq. (11). Applying the inverse Fourier transform with the electric field from Eq. (7), we can obtain the compressed pulse

$$E(t') = \left(\frac{ib}{2\pi\tau^2}\right)^{1/2}\exp\left[-i\frac{1}{2}b\left(\frac{t'}{\tau}\right)^2\right]\exp(i\omega_0)t'$$
$$\times\int A_2\exp\left[-\frac{1}{2}\left(\frac{t}{\tau}\right)^{2m} - \frac{1}{2}\left(\frac{t}{\tau_{\mathrm{eff}}}\right)^2\right]$$
$$\times\exp\left\{i\left[\Phi_{\mathrm{NL}}(t) - \phi_{\mathrm{SPM}}(t)\right]\right\}\exp\left(\frac{ibtt'}{\tau^2}\right)\mathrm{d}t. \quad (12)$$

If we neglect the nonlinear chirp and phase modulation in the integral, the compressed pulse envelope is a Fourier transform of the input-pulse envelope.[6] Thus a Gaussian-envelope pulse, which can be obtained through gain-narrowing, is the best choice for compression, and the compressed pulse is still Gaussian. A higher-order super-Gaussian-envelope pulse, which is almost a square pulse, is not a good choice for pulse compression. Its Fourier transform is a sinclike function that carries gross structure in the pedestal. The nonlinear chirp $\phi_{\mathrm{NL}}(t)$ and phase modulation $\phi_{\mathrm{SPM}}(t)$ diffuse the light in time and form the pedestal of the compressed pulse.

B. Numerical Example

Figure 8(a) shows the power spectrum of a chirped super-Gaussian pulse [Eq. (6)] with parameters $\tau = 75$ ps, $m = 25$, $b = 236$, and a small amount of phase variation $\phi_{\mathrm{NL}}(t) = -(t/\tau)^3 - 4(t/\tau)^4$. These values were chosen so that the frequency spectrum would match the experimental one observed at the exit of the fiber. The bandwidth is 37 Å (FWHM). The term $-(t/\tau)^3$ makes the spectrum asymmetric, and the term $-4(t/\tau)^4$ makes the spectrum more peaked near two edges. Figure 8(b) shows the intensity profile of the compressed pulse with a pulse width of 1.6 ps (FWHM); Fig. 8(b) can be compared with Fig. 4(b). The gross pedestal is the result of its original chirped pulse profile (nearly square top) and the nonlinear chirp. Figure 8(c) shows the power spectrum of an amplified pulse [Eq. (7)] with parameters $\tau = 150$ ps, $\tau_{\mathrm{eff}} = 60$ ps, $m = 25$, $b = 472$, and the same $\phi_{\mathrm{NL}}(t)$. The profile is near Gaussian with a bandwidth of 13 Å (FWHM). Figure 8(d) shows the final compressed pulse with a pulse width of 1.6 ps (FWHM). The pedestal is significantly suppressed by spectral gain narrowing, as was shown by Perry *et al.*[12] Neglecting the long-duration satellite pulses, the calculated gain-narrowed spectrum and pulse shape shown in Figs. 8(c) and 8(d) are similar to those observed experimentally, shown in Figs. 5(a) and 5(b).

To illustrate the roles of frequency mismatch and SPM in a CPA laser, Fig. 9 shows the intensity profile of the final compressed pulse under a variety of conditions with the same chirp parameters as those used for Fig. 8(d). Figure 9(a) shows the gain-frequency-matched case with SPM. In this figure an enhanced pedestal level is clearly shown even though the total peak B-integral value is only 2.0. This can occur quite easily in a multiple-pass regen-

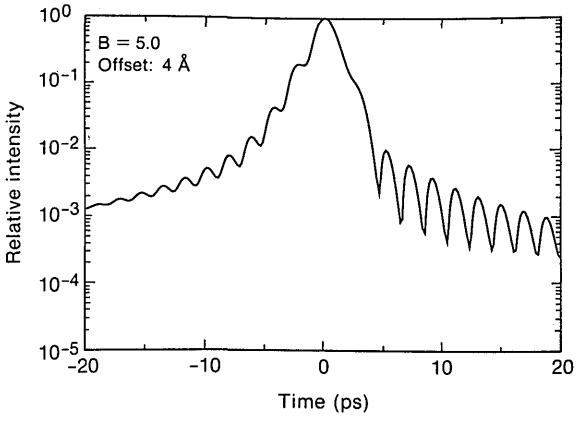

Fig. 10. Calculated compressed pulse with conditions similar to those of the pulse shown in Fig. 3(a). The initial pulse, with a chirped-frequency bandwidth of 20 Å and a duration of 150 ps, is amplified with a frequency mismatch of 4 Å at $B = 5.0$.

erative amplifier near gain saturation when the laser intensity is high and accumulates SPM in each pass.[17] For example, for a laser pulse at $\lambda = 1053$ nm with a peak intensity equal to 1 GW/cm^2 that travels through an amplifier with a nonlinear index of refraction $n_{2E} = 1.2 \times 10^{-13}$ esu (for Nd^{+3}-doped phosphate glass Q98) and with an amplifier length $L = 115$ mm, the peak SPM is equal to 0.22. Thus, at this intensity level, a laser pulse will accumulate a significant amount of SPM in several passes through the amplifier, and the resulting new frequency chirp will increase the pedestal of the compressed pulse in the final compression stage. Figure 9(b) shows the gain-frequency mismatched case (4-Å mismatch) without SPM. The laser pulse is not well compressed because of the poor pulse-shaping condition, as stated above.

Figure 10 shows an example that is similar to the case shown in Fig. 3(a). A chirped pulse with a 20-Å bandwidth, a 150-ps pulse duration, and a frequency mismatch between the regenerative amplifier and the Nd:YLF oscillator of 4 Å is modeled with a B integral equal to 5.0. A significant enhancement of the pedestal is seen.

5. CONCLUSION

We have discussed four different contributions to the pedestal that is associated with a CPA laser system and have investigated techniques to reduce them, leading to the production of high-intensity-contrast (>10^5:1) 0.9-ps Gaussian pulses. The pedestal consists of (a) a background pedestal that results from SPM during the operation of the regenerative amplifier near gain saturation, (b) étalon effects, (c) pulse wings, and (d) satellite pulses. The last two result from the nonlinear chirp and square-top envelope generated in the optical fiber. The pulse is switched out before gain saturation so that further frequency modulation in the regenerative amplifier is avoided. The pulse wings are suppressed by gain narrowing in the spectral line-center-matched regenerative amplifier. A saturable absorber is used to suppress the satellite pulses and further reduce the pedestal.

These results suggest a method for increasing the energy and temporal and focal qualities in a CPA laser. The laser pulse from the Nd:YLF oscillator will first be chirped by the fiber and then be injected directly into the regenerative amplifier without further stretching. The resulting 1-mJ-level pulse will then be compressed by the first compression-grating pair and will pass through the saturable absorber, so that the pedestal is removed. This low-pedestal pulse will be restretched and chirped in an expansion-grating pair[7] and be injected into the amplifier chain. After amplification the chirped pulse will be perfectly compressible in the final compression-grating pair, since the expansion- and compression-grating pairs have opposite functions and will be separated by the same distance. Without suffering any higher-order chirp this pulse can be stretched to an arbitrary chirp ratio in order to gain more energy and to reach the same intensity-ratio increase after compression. The limiting factors are the size of the gratings and the space required for grating separation.[4]

With this pedestal reduction, high-intensity-contrast picosecond pulses with intensities exceeding 10^{16} W/cm^2 can be produced with the current system, with higher intensities available for larger gratings. The results of this work make possible the study of high-intensity ultrashort laser plasma interactions with a fiber–grating CPA system. It is important to note, though, that chirped pulses with Gaussian envelopes can undergo SPM if the total B integral is of the order of 2,[22] and this factor must be taken into account in the design of future high-power CPA systems.

Note added in proof. Recent results of Yamakawa *et al.*[23] show the reduction of the prepulse to main pulse intensity to better than 1/900 through the use of a saturable absorber immediately after the fiber.

ACKNOWLEDGMENTS

We thank D. L. Brown, J. Kelly, Z-W. Li, and M. C. Richardson for expert technical assistance.

This work was supported by the U.S. Department of Energy Division of Inertial Fusion under agreement DE-FC03-85DP40200 and by the Laser Fusion Feasibility Project at the Laboratory for Laser Energetics, which has the following sponsors: Empire State Electric Energy Research Corporation, New York State Energy Research and Development Authority, Ontario Hydro, and the University of Rochester.

Y.-H. Chuang, D. D. Meyerhofer, and S. Uchida are also with the Department of Mechanical Engineering, University of Rochester, Rochester, New York 14623.

S. Augst, H. Chen, and J. Peatross are also with the Department of Physics and Astronomy, University of Rochester, Rochester, New York 14623.

REFERENCES

1. M. M. Murnane, H. C. Kapteyn, and R. W. Falcone, "High-density plasmas produced by ultrafast laser pulses," Phys. Rev. Lett. **62,** 155 (1989).
2. O. L. Landen, E. M. Campbell, and M. D. Perry, "X-ray characterization of picosecond laser plasmas," Opt. Commun. **63,** 253 (1987).
3. J. A. Cobble, G. A. Kyrala, A. A. Hauer, A. J. Taylor, C. C. Gomez, N. D. Delamater, and G. T. Schappert, "Kilovolt x-ray spectroscopy of a subpicosecond-laser-excited source," Phys. Rev. A **39,** 454 (1989).
4. P. Maine, D. Strickland, P. Bado, M. Pessot, and G. Mourou, "Generation of ultrahigh peak power pulses by chirped pulse amplification," IEEE J. Quantum Electron. **24,** 398 (1988).
5. G. P. Agrawal, *Nonlinear Fiber Optics* (Academic, Boston, Mass., 1989), Chaps. 4 and 6.
6. E. B. Treacy, "Optical pulse compression with diffraction gratings," IEEE J. Quantum Electron. **QE-5,** 454 (1969).
7. M. Pessot, P. Maine, and G. Mourou, "1000 Times expansion/compression of optical pulses for chirped pulse amplification," Opt. Commun. **62,** 419 (1987).
8. A. E. Siegman, *Lasers* (University Science, Mill Valley, Calif., 1986), Chaps. 5, 9, and 10.
9. R. H. Stolen, J. Botineau, and A. Ashkin, "Intensity discrimination of optical pulses with birefringent fibers," Opt. Lett. **7,** 512 (1982); B. Nikolaus, D. Grischkowsky, and A. C. Balant, "Optical pulse reshaping based on the nonlinear birefringence of single-mode optical fibers," Opt. Lett. **8,** 189 (1983); N. J. Halas and D. Grischkowsky, "Simultaneous optical pulse compression and wing reduction," Appl. Phys. Lett. **48,** 823 (1986).
10. H. Kubota and M. Nakazawa, "Compensation of nonlinear chirp generated by self-steepening using third order dispersion of a grating pair," Opt. Commun. **66,** 79 (1988).
11. J. P. Heritage, R. N. Thurston, W. J. Tomlinson, A. M. Weiner, and R. H. Stolen, "Spectral windowing of frequency-modulated

optical pulses in a grating compressor," Appl. Phys. Lett. **47,** 87 (1985).
12. M. D. Perry, F. G. Patterson, and J. Weston, "Spectral shaping in chirped-pulse amplification," Opt. Lett. **15,** 381 (1990).
13. J. P. Heritage, A. M. Weiner, R. J. Hawkins, and O. E. Martinez, "Stabilized pulse compression by multiple-order stimulated Raman scattering with group velocity dispersion," Opt. Commun. **67,** 367 (1988).
14. H. Roskos, A. Seilmeier, W. Kaiser, and J. D. Harvey, "Efficient high-power optical pulse compression with logarithmic wing analysis," Opt. Commun. **61,** 81 (1987).
15. J. S. Coe, P. Maine, and P. Bado, "Regenerative amplification of picosecond pulses in Nd:YLF: gain narrowing and gain saturation," J. Opt. Soc. Am. B **5,** 2560 (1988).
16. W. J. Tomlinson, "Curious features of nonlinear pulse propagation in single-mode optical fibers," Opt. News **15**(1), 7 (1989).
17. W. Zinth, A. Laibereau and W. Kaiser, "Generation of chirp-free picosecond pulses," Opt. Commun. **22,** 161 (1977).
18. J. D. McMullen, "Analysis of compression of frequency chirped optical pulses by a strongly dispersive grating pair," Appl. Opt. **18,** 737 (1979).
19. O. E. Martinez, "Grating and prism compressors in the case of finite beam size," J. Opt. Soc. Am. B **3,** 929 (1986).
20. G. Albrecht, A. Antonetti, and G. Mourou, "Temporal shape analysis of Nd^{3+}:YAG active passive mode-locked pulses," Opt. Commun. **40,** 59 (1981).
21. B. Kopainsky, W. Kaiser, and K. H. Drexhage, "New ultrafast saturable absorbers for Nd: lasers," Opt. Commun. **32,** 451 (1980).
22. Y. H. Chuang, J. Peatross, and D. D. Meyerhofer, "Modeling the pedestal in a chirped-pulse-amplification laser," in *Proceedings of the Short-Pulse, High-Intensity Lasers and Applications Conference,* Proc. Soc. Photo-Opt. Instrum. Eng. (to be published).
23. K.-I. Yamakawa, C. P. J. Barty, H. Shiraga, and Y. Kato, "Generation of a high-energy picosecond laser pulse with a high contrast ratio by chirped pulse amplification," IEEE J. Quantum Electron. (to be published).